Research Article

Amir Bahrami, Klaas De Kinder, Zhiyu Li and Christophe Caloz*

Space-time wedges

Abstract: Space-time–modulated systems have attracted significant interest over the past decade due to their ability to manipulate electromagnetic waves in unprecedented ways. Here, we introduce a new type of space-time–modulated structure, the *space-time wedge*, consisting of two interfaces moving at different velocities, which results in either closing or opening wedges. Using moving boundary conditions, we derive closed-form solutions for the scattering of electromagnetic waves in such a wedge and leverage these solutions to unveil the underlying physics, including multiple space-time scattering and Doppler shifting. The space-time wedge holds potential for various optical and photonic applications.

1 Introduction

Generalized Space-Time Engineered Modulation (GSTEM) systems, or GSTEMs for short, are structures whose properties are modulated in both space and time by an external drive [1]. The modulation can take various forms, including electronic, optical, acoustic, mechanical, thermal, and chemical [2]–[6]. This modulation typically manifests as a traveling or standing wave perturbation in one of the medium's constitutive parameters. Therefore, GSTEM systems are best classified based on their modulation velocity regime. The most common regime is instantaneous

modulation (or infinite velocity) [7], [8], which enables a wide range of applications and physical phenomena, such as time reversal [8], [9], time refraction [10]–[12], breaking of fundamental bounds [13], beam splitting [14], photon generation [15] and cooling [16], inverse prism [17], four-dimensional metamaterials [18], perfect absorption [19], parametric amplification [20], temporal impedance matching [21], and temporal aiming [22]. In recent years, this regime has also been explored beyond classical physics [23]–[27]. The modulation velocity can also vary uniformly, ranging from subluminal to superluminal speeds [28]–[32], which introduces additional novel phenomena, including Doppler shifting [29], [33], [34], magnetless nonreciprocity [35]–[37], space-time reversal [38], dynamic diffraction [39], asymmetric bandgaps [29], [40], [41] and isolation [42], light deflection [43]–[45], quantum cosmological analogs [46], and shock-wave production [47]. Finally, the modulation velocity can be nonuniform, where acceleration enables phenomena such as radiation from moving mirrors [48], photon emission [49], chirping [50], light bending [51], and gravity analogs [52].

GSTEMs encompass several fundamental structures, including interfaces, slabs, space-time crystals, and space-time metamaterials. Interfaces serve as the core building blocks of all GSTEMs [53], [54]. Slabs are formed by stacking two interfaces moving at the same velocity [55], [56]. Space-time crystals result from the periodic repetition of slabs with different properties [29]. Finally, space-time metamaterials are created by reducing the spatial and temporal periods of these crystals to subwavelength and subperiod scales [29], [40].

Here, we introduce a new fundamental class of GSTEM structures, the *space-time wedge*. A space-time wedge is formed by combining two space-time interfaces with different velocities, corresponding to a wedge- or triangular-shaped structure in the space-time diagram. In a purely spatial representation, with space as the abscissa and a property (such as refractive index or potential) as the ordinate, these wedges correspond to shrinking (closing wedge) or expanding (opening wedge) slabs.

The paper is organized as follows. Section 2 introduces the concept of space-time wedges as an extension of conventional space-space wedges. Then, Section 3 presents a classification of all possible types of space-time wedges. Next,

*Corresponding author: Christophe Caloz, KU Leuven, Leuven, 3000, Belgium, E-mail: christophe.caloz@kuleuven.be.
https://orcid.org/0000-0003-0502-8435
Amir Bahrami and Klaas De Kinder, KU Leuven, Leuven, 3000, Belgium, E-mail: amir.bahrami@kuleuven.be (A. Bahrami),
klaas.dekinder@kuleuven.be (K. De Kinder).
https://orcid.org/0000-0001-9472-4429 (A. Bahrami).
https://orcid.org/0009-0003-7646-9016 (K. De Kinder)
Zhiyu Li, Xi'an Jiaotong University, Xi'an, 710049, China.
https://orcid.org/0000-0002-0110-0850

Section 4 provides the resolution strategy to determine the scattered waves at a space-time wedge. Then, Section 5 addresses the scattering problem at dielectric space-time wedges and provides two representative examples for such phenomena. Next, Section 6 describes the frequency transitions observed in the scattered waves. Section 7 tackles the scattering problem at impenetrable wedges as a special case of dielectric wedges, with examples showcasing space-time multiple scattering effects and Doppler frequency shifts. Finally, Section 8 discusses experimental implementations and potential applications.

2 Space-time wedge concept

The space-time wedge must be clearly distinguished from the conventional, "space-space" wedge, in terms of both its structure and its operation. Let us, therefore, describe both wedges, with the help of Figure 1.

Figure 1(a) shows the geometry of a space-space wedge. Such a wedge is a dielectric or metallic structure with one or more sharp vertices [57]. When light impinges on a vertex, it diffracts, while when it impinges on an edge, it undergoes

Figure 1: Wedge structure, consisting of two interfaces separating two media of different refractive indices, n_1 and n_2, and related scattering. (a) Conventional space-space closing wedge with (b) diffraction due to vertex excitation and refraction due to edge excitation. (c) Space-time wedge, with two interfaces moving at different velocities, v_1 and v_2, and colors corresponding to different frequencies, and (d) related space-index perspective.

Snell's refraction, as shown in Figure 1(a) and (b). The optical behavior of space-space wedges, including diffraction and refraction phenomena, has been extensively studied and is considered a canonical problem in electromagnetic theory [3].

Figure 1(c) shows a space-time wedge. This wedge is obtained by replacing the space (x) ordinate of the space-space wedge in Figure 1(a) by time (ct). The resulting structure consists of two interfaces moving at different velocities, whose space-index representation is shown in Figure 1(d).[1] Unlike the space-space wedge, the space-time wedge does not involve diffraction, due to causality. In contrast, it induces Doppler shifting[2] in both reflection and transmission, which can be either upshifted or downshifted depending on the velocity and properties of the medium.

In this paper, we restrict ourselves to space-time wedges with *two edges* (and one vertex), originating at the spatial points z_1 and z_2, as shown in Figure 1(d). However, an analogous approach may be applied to the problem of wedges with two or three vertices, and even to the problem of polygonal structures with more edges.

3 Classification

Space-time wedges, as described in Section 2, are composed of two space-time interfaces. These interfaces can be classified according to their velocity, v. The velocity may be subluminal, interluminal, or superluminal. The subluminal and superluminal velocities correspond to regimes $v < \min\{c/n_1, c/n_2\}$ and $v > \max\{c/n_1, c/n_2\}$, respectively, while the interluminal velocities correspond to the regime $\min\{c/n_1, c/n_2\} < v < \max\{c/n_2, c/n_2\}$. The scattering behavior of interfaces in the subluminal and superluminal regimes have been extensively studied [45], [54]. In contrast, investigations of scattering in the interluminal regime remain limited to specific cases [58], [59].

The wedges can be classified according to the velocity regimes (subluminal, interluminal, or superluminal) of their two interfaces and whether the wedge is opening or closing with time. Figure 2 represents all the possible types of wedges together with the assumed direction of
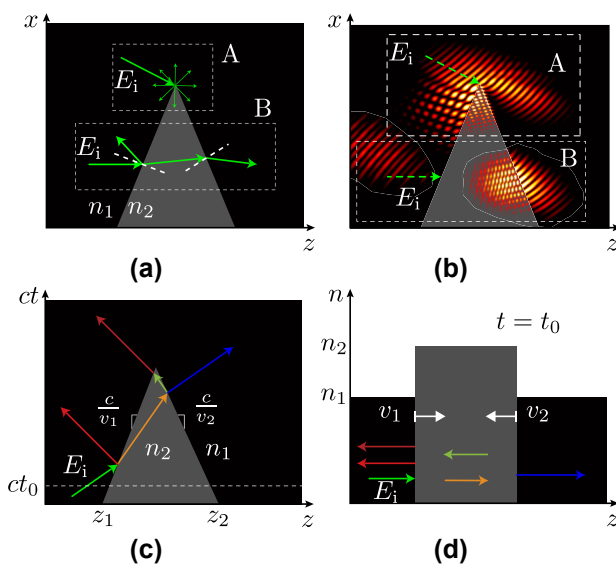
---

1 In quantum physics, this structure would be interpreted as a widening or narrowing potential barrier or well.

2 The reflection Doppler shifting is well-known, with up/down-shifting for an approaching/receding object. The transmission Doppler shifting is less known; it depends not only on the velocity of the object's interface but also on its refractive index contrast. This may be understood in terms of the pulse expansion and compression described in Ref. [53].
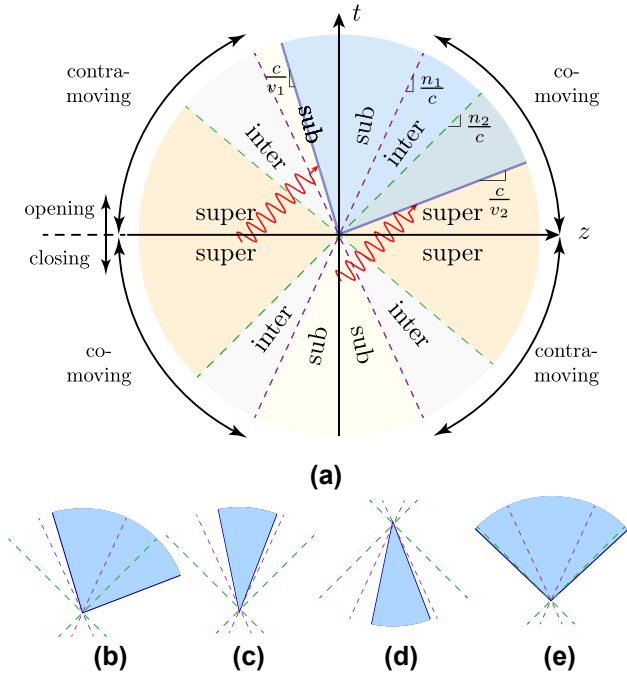
(a)

(b)   **(c)**   **(d)**   **(e)**

Figure 2: Classification of space-time wedges. (a) Generic operating regimes and examples of (b) subluminal/superluminal opening, (c) subluminal/subluminal opening, (d) subluminal/subluminal closing, and (e) superluminal/superluminal opening wedges.

the incident wave ($\pm c/n_1$). For instance, the wedge represented in Figure 2(a), and isolated in Figure 2(b), corresponds to an opening wedge, whose left interface is subluminal and contra-moving with respect to the incident wave, and right interface is superluminal and comoving with respect to the incident wave. Such a configuration will be hereafter referred to as a subluminal/superluminal opening wedge. Similarly, Figure 2(c)–(e) correspond to subluminal/subluminal opening, subluminal/subluminal closing, and superluminal/superluminal opening wedges, respectively. This classification results in 78 distinct scattering configurations (see Section 1 in Ref. [60] for all the configurations).

4 Resolution frame selection

Scattering problems at moving interfaces are commonly addressed using a method known as frame-hopping [61]. This approach simplifies the problem by transforming coordinates from the laboratory frame to the comoving frame, reducing it to the scattering at a stationary interface. Once the scattering coefficients are calculated in this comoving frame, the results are then transformed back to the laboratory frame. This technique is particularly effective for

analyzing scenarios involving moving interfaces and slabs [29]. However, in the case of wedges, we encounter a complication: wedges entail two velocities that are generally not equal.[3] Consequently, there is no frame where both interfaces are stationary.[4] As a result, we must tackle the problem within the laboratory frame and use moving boundary conditions.

5 Scattering formulas

According to Figure 1(c), the incident (ψ_i), transmitted (ψ_t), and reflected (ψ_r) waves in medium 1 (surrounding of the wedge) are traveling waves, which may be written as

$$E_x^i = \psi_i\left[\frac{z}{u_1} - t\right], \tag{1a}$$

$$E_x^t = \psi_t\left[\frac{z}{u_1} - t\right] \tag{1b}$$

and

$$E_x^r = \psi_r\left[\frac{z}{u_1} + t\right], \tag{1c}$$

where $u_1 = c/n_1$ is the speed of light in medium 1, where we have assumed that the incident wave is launched in medium 1. On the other hand, waves in medium 2 (wedge) are a superposition of forward (ψ_f) and backward (ψ_b) traveling waves, which may be written as

$$E_x^w = \psi_f\left[\frac{z}{u_2} - t\right] + \psi_b\left[\frac{z}{u_2} + t\right], \tag{2}$$

where $u_2 = c/n_2$ is the speed of light in medium 2. We have used square brackets, [·], to indicate the arguments of the wave functions (ψ_i, ψ_t, ψ_r, ψ_f, and ψ_b) in Eqs. (1) and (2). In the forthcoming examples, we will use Gaussian modulated pulse for the incidence, viz., $\psi_i[z/u_1 - t] = \exp(i\omega_i(z/u_1 - t)) \exp(-\frac{(z/u_1-t)^2}{\sigma^2})$, with ω_i being the incident frequency and σ the width of the Gaussian pulse.

    We now apply the moving boundary conditions at each interface of the wedge. These conditions prescribe the continuity of $\mathbf{E} + \mathbf{v_1} \times \mathbf{B}$ and $\mathbf{H} - \mathbf{v_1} \times \mathbf{D}$ for the first interface and $\mathbf{E} + \mathbf{v_2} \times \mathbf{B}$ and $\mathbf{H} - \mathbf{v_2} \times \mathbf{D}$ for the second interface. This leads to a pair of recurrent equations whose combination provides the sought-after scattered wave solutions (see Section 2 in Ref. [60] for detailed derivations)

---

3 In the limiting case of equal velocities, the wedge reduces to a slab.
4 This situation is akin to two cars moving in opposite directions, making it impossible to follow both simultaneously.

$$\psi_t\left[\frac{z}{u_1} - t\right]$$

$$= T_{12}T_{21}H\sum_{p=0}^{\infty} R^{2p}D^p\psi_i\underbrace{\left[\Delta\phi_p + HD^p\left(\frac{z}{u_1} - t\right)\right]}_{\Phi_t} \quad (3a)$$

and

$$\psi_r\left[\frac{z}{u_1} + t\right] = R\frac{M_{11}^-}{M_{11}^+}\psi_i\left[\phi_0' - \frac{M_{11}^-}{M_{11}^+}\left(\frac{z}{u_1} + t\right)\right]$$

$$- T_{12}T_{21}H'\sum_{p=0}^{\infty} R^{2p+1}D'^p\psi_i$$

$$\times \underbrace{\left[\Delta\phi_p' + H'D'^p\left(\frac{z}{u_1} + t\right)\right]}_{\Phi_r} \quad (3b)$$

with

$$\Delta\phi_p = A + BC\left(\frac{1-D^p}{1-D}\right) + BD^p\left(\frac{z_2}{u_2} - \frac{z_2 M_{22}^-}{u_1 M_{21}^-}\right), \quad (3c)$$

$$\phi_0' = \frac{z_1}{u_1}\left(1 + \frac{M_{11}^-}{M_{11}^+}\right) \quad (3d)$$

and

$$\Delta\phi_p' = A' + B'C'\left(\frac{1-D'^p}{1-D'}\right) + B'D'^p\left(\frac{z_1}{u_2} - \frac{z_1 M_{12}^+}{u_1 M_{11}^+}\right), \quad (3e)$$

where

$$R = \frac{\eta_2 - \eta_1}{\eta_2 + \eta_1}, \quad T_{ij} = \frac{2\eta_j}{\eta_i + \eta_j}, \quad M_{ij}^\pm = 1 \pm \frac{v_i}{u_j}, \quad (3f)$$

$$A = \frac{z_1}{u_1} - \frac{z_1}{u_2}B, \quad A' = \frac{z_1}{u_1} - \frac{z_2}{u_2}B' + \frac{z_2 - z_1}{u_2}\frac{M_{11}^-}{M_{12}^-}, \quad (3g)$$

$$B = \frac{M_{11}^-}{M_{12}^-}, \quad B' = -\frac{M_{11}^- M_{22}^-}{M_{12}^- M_{22}^+}, \quad (3h)$$

$$C = \frac{z_2}{u_2} - \frac{z_1}{u_2}D + \frac{z_2 - z_1}{u_2}\frac{M_{22}^-}{M_{22}^+}, \quad (3i)$$

$$C' = \frac{z_1}{u_2} - \frac{z_2}{u_2}D' - \frac{z_2 - z_1}{u_2}\frac{M_{12}^+}{M_{12}^-}, \quad D = D' = \frac{M_{12}^+ M_{22}^-}{M_{12}^- M_{22}^+} \quad (3j)$$

and

$$H = \frac{M_{22}^- M_{11}^-}{M_{21}^- M_{12}^-}, \quad H' = -\frac{M_{12}^+ M_{11}^- M_{22}^-}{M_{11}^+ M_{12}^- M_{22}^+}. \quad (3k)$$

In these relations, R and T_{ij} correspond to the conventional reflection and transmission coefficients at a stationary interface (from media 1 to 2, resp. i to j) with η_1 and η_2 being the impedance of medium 1 and 2, M_{ij} is a term related to Doppler shifting, and $\Delta\phi_p$ and $\Delta\phi_p'$ together with the parameters given in Eqs. (3g)–(3k) account for the accumulated phase shifts for the transmitted and the reflected waves, respectively.

Equations (3) may be physically interpreted as follows. The summation terms in Eqs. (3a) and (3b), running from 0 to ∞, represent the *multiple space-time scattering events* occurring within the wedge (see Figure 1(d)). Let us first analyze the reflected wave, Eq. (3b). The first, summation-less term in the right-hand side of Eq. (3b), which has no equivalent in Eq. (3a), corresponds to the initial reflection at the first interface, while the second term, with the factor $T_{12}T_{21}H'$ describes transmission across the wedge, with the effect of the multiple scattering within the wedge being accounted for by the summation including reflection R^{2p+1} and Doppler shifting D'^p. Similar observations can be made with the transmitted wave, Eq. (3a), since the corresponding relation is essentially similar to the reflected wave.

Figure 3 shows the space-time evolution and frequency spectra of the scattering phenomena described by Eqs. (3a) and (3b). Figure 3(a) shows the scattering behavior of a closing wedge. Upon encountering the initial interface, a portion of the incident wave is reflected ($E_{r,1}$) with a Doppler
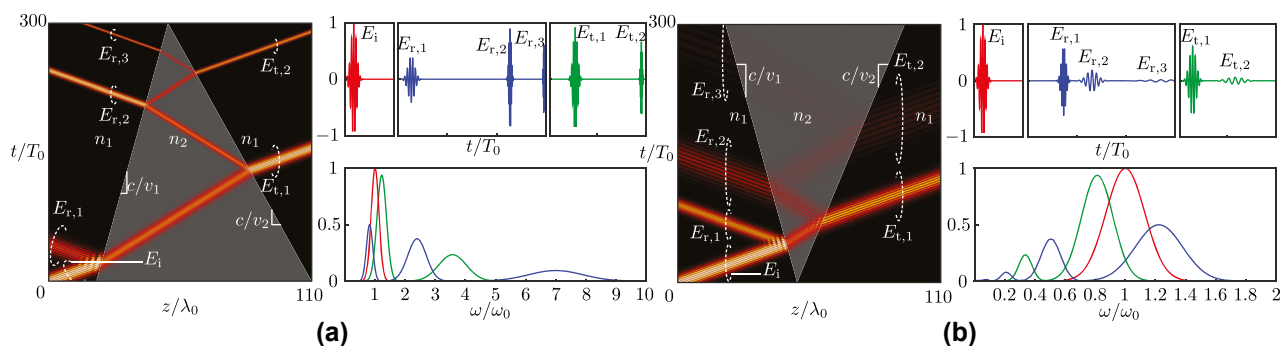

Figure 3: Scattering at a dielectric wedge separating two media, of permittivities $\epsilon_1 = 1$ and $\epsilon_2 = 3$. (a) Closing wedge, with $v_1 = 0.1c$ and $v_2 = -0.2c$, and (b) opening wedge, with $v_1 = -0.1c$ and $v_2 = 0.15c$.

downshift, attributed to the interaction with a comoving interface. Within the wedge, the wave undergoes multiple contramoving space-time reflections, resulting in successive Doppler upshifting. In contrast, Figure 3(b) presents the scattering behavior of an opening wedge. Here, the initial reflection ($E_{r,1}$) exhibits upshifting. As the wave propagates within the wedge, it experiences successive Doppler downshifting due to repeated interactions with the comoving interfaces.

6 Frequency transitions

Space-time wedges produce scattered waves with multiple new frequencies, as illustrated in Figure 3. The related frequency shifts result from multiple Doppler shifts occurring during interactions with the wedge interfaces. The frequency change after each scattering event can be calculated by taking the derivative of the arguments in Eqs. (3a) and (3b), viz.,

$$f_t = \frac{\partial \Phi_t}{\partial t} = H D^p \tag{4a}$$

and

$$f_r = \frac{\partial \Phi_r}{\partial t} = H' D'^p, \tag{4b}$$

where p denotes the number of scattering events. After each interaction, the frequency of the wave is either upshifted or downshifted, depending on whether it interacts with a contramoving or a comoving interface, respectively.

These frequency transformations (Eq. (4)) can be graphically represented and validated in the "*transition diagrams*" shown in Figure 4, where Figure 4(a) and (b) corresponds to the closing and opening wedges of Figure 3(a) and (b). The transition diagrams of Figure 4 may be progressively constructed by following the wave scattering events in Figure 3. Let us consider the closing wedge case. The incident wave starts at the point $(k/k_0, \omega/\omega_0) = (1, 1)$ (red dot). Then, it experiences a first pair of transitions at the interface 1, and hence under the angle v_1: a reflection transition in medium n_1 (lowest blue dot) and a transmission transition into medium n_2 (lowest black dot). Next, the transmitted wave (lowest black dot) crosses the wedge and incurs a new scattering event and a new transition pair at the interface 2, under the angle v_2: a transmission transition into medium n_1 (lowest green dot) and a reflection transition in medium n_2 (second lowest black dot). The next scattering points, and Figure 4(b), follow the same logic. Note that the closing wedge gradually increases the reflected and transmitted frequencies—or photon energies—while the opening wedge constantly decreases these frequencies or energies.
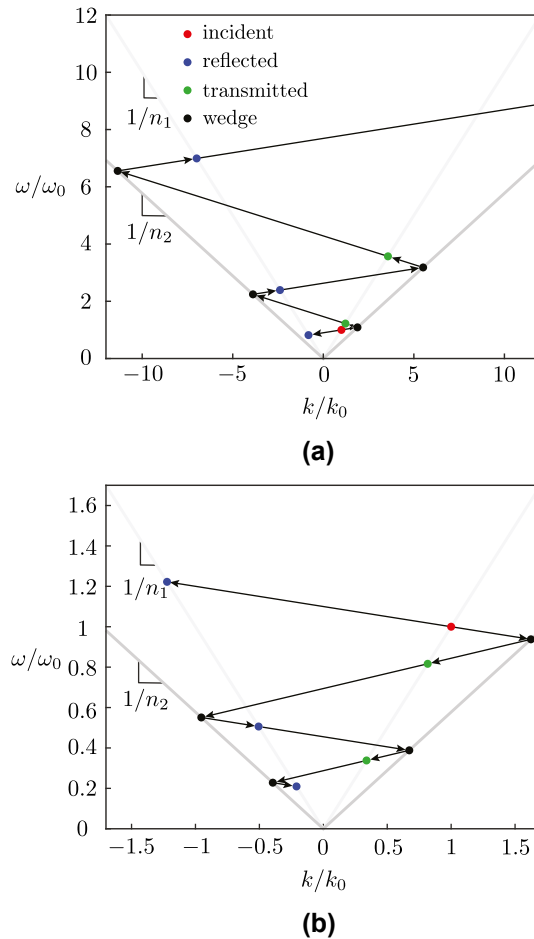

(a)

(b)

Figure 4: Transition diagrams for the cases of (a) a closing wedge with velocities $v_1 = 0.1c$ and $v_2 = -0.2c$ (Figure 3(a)) and (b) a closing wedge with velocities $v_1 = -0.1c$ and $v_2 = 0.15c$ (Figure 3(b)).

7 Impenetrable wedges

Having examined wave scattering and propagation in space-time wedges formed by modulated dielectric materials, we now focus on a particular case of space-time wedge, a space-time wedge with its exterior (medium 1) being impenetrable.[5] In contrast to dielectric wedges, where waves propagate and scatter *across* the space-time structure, the impenetrable space-time wedge entirely confines waves within its interior once excited there. The scattering and propagation of electromagnetic waves in the structure can be found by applying *Perfect Electric Conductor (PEC) moving boundary conditions* at each interface [29], viz., $\mathbf{E} + \mathbf{v_1} \times \mathbf{B} = 0$ at the first interface and $\mathbf{E} + \mathbf{v_2} \times \mathbf{B} = 0$ at

---

5 A space-time wedge with its *interior* (medium 2) being impenetrable is possible but fairly trivial, as its scattering reduces to a single (Doppler-shifted) reflection.
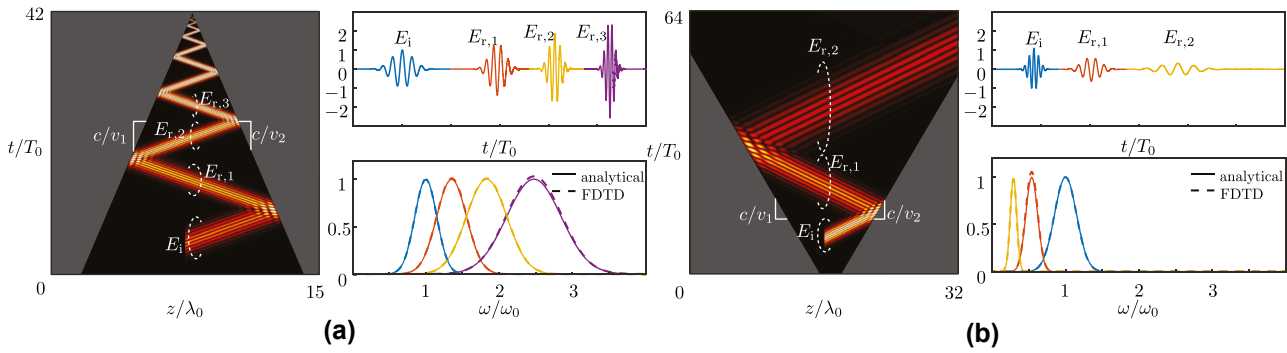
Figure 5: Scattering at PEC space-time wedges shown in space-time diagrams (left panels) with corresponding time-domain waveforms and spectra (right panels) for (a) a closing wedge, with interfaces moving at velocities $v_1 = -v_2 = 0.15c$ and (b) an opening wedge with interfaces moving at velocities $v_1 = -v_2 = -0.3c$.

the second interface. This operation results in a recursive equation, whose solution is the multiple scattering expression[6] [60]

$$
E_x^{\mathrm{w}} = \sum_{p=0}^{\infty} (R_1 R_2)^{p+1} \psi_{\mathrm{i}} \left[\Delta\phi_p + (R_1 R_2)^{p+1} \left(\frac{z}{u_1} - t \right) \right]
$$
$$
- \sum_{p=0}^{\infty} R_1^p R_2^{p+1} \psi_{\mathrm{i}} \left[\Delta\phi_p' - R_1^p R_2^{p+1} \left(\frac{z}{u_1} + t \right) \right], \tag{5}
$$

where

$$
R_1 = \frac{M_{11}^+}{M_{11}^-} \tag{6a}
$$

and

$$
R_2 = \frac{M_{21}^-}{M_{21}^+} \tag{6b}
$$

are the conventional scattering coefficients at a PEC interface moving at velocity v_1 and v_2, respectively [56].

Figure 5 shows the space-time evolution and frequency spectra of scattering at space-time wedges with impenetrable (PEC) interfaces, computed by Eq. (5) and validated by FDTD simulation [50]. Unlike the dielectric wedges discussed in Section 5, where the wave may escape the wedge, the wave in the PEC wedges remain confined within the structure. Figure 5(a) depicts the scattering in a closing PEC wedge, where the wave constantly interacts with contramoving interfaces, causing a gradual frequency upshift. Conversely, Figure 5(b) shows scattering in an opening PEC

wedge, where the wave gradually reflects off comoving interfaces, resulting in a gradual frequency downshift.[7]

8 Conclusions

The paper has introduced and explored the concept of space-time wedges, a novel type of GSTEM. We have demonstrated the unique scattering phenomena that occur in these structures, including multiple Doppler frequency shifts and multiple space-scattering scattering. We have classified the various types of space-time wedges based on their velocity regimes and derived closed-form solutions for the scattered waveforms. Such a wedge may have various applications in dynamic classical optical and quantum photonic devices, such as frequency converters, modulators, multiplexers, wave or particle traps, and photon heating and cooling systems.

Wedge structures can be implemented by finely loading an artificial transmission line with varactor diodes. As each diode is triggered, typically from an external control circuit, the local properties of the transmission line change. By sequentially switching these diodes in a specific pattern – for example, from left-to-right (center-to-left) and right to left (center-to-right) – it is possible to create two approaching (receding) interfaces on the transmission line. This corresponds to the realization of closing (opening) space-time wedges.

---

6 Note that Eq. (5) is *not* a particular case of Eqs. (3a) and (3b). This is because reflection in the PEC wedge occurs exclusively within the wedge structure, whereas the dielectric wedge equations apply only outside the wedge.

7 The fact that the spectral magnitudes in Figure 5 are all equal, whereas the envelopes of the corresponding temporal pulses are not, might *a priori* seem contradictory. However, this is explained by the Doppler effect. In the time domain, both the magnitude and the frequency of the incident pulse are scaled by the Doppler effect, by some factor a, as $E(t) \to aE(at)$ [54]. The corresponding Fourier transform, $\tilde{E}(\omega) = \mathcal{F}(\omega/a)$, reveals that the spectral magnitude is equal to the temporal magnitude before Doppler shifting.

Author contributions: AB performed the bulk of the work. KDK assisted with the elaboration of the transition diagram concept (Figure 4). ZL constructed the classification diagram (Figure 2). CC has supervised the work. All authors have accepted responsibility for the entire content of this manuscript and approved its submission.

Conflict of interest: Authors state no conflict of interest.

Data availability: The datasets generated during and/or analyzed during the current study are available from the corresponding author on a reasonable request.

References

[1] C. Caloz, Z.-L. Deck-Léger, A. Bahrami, O. C. Vicente, and Z. Li, "Generalized space-time engineered modulation (GSTEM) metamaterials: a global and extended perspective," *IEEE Antenn. Propag. Mag.*, vol. 65, no. 4, pp. 50−60, 2023.

[2] W. T. Rhodes, "Acousto-optic signal processing: convolution and correlation," *Proc. IEEE*, vol. 69, no. 1, pp. 65−79, 1981.

[3] B. E. Saleh and M. C. Teich, *Fundamentals of Photonics*, Hoboken, New Jersey, USA, John Wiley & Sons, 2019.

[4] L. Xu, G. Xu, J. Huang, and C.-W. Qiu, "Diffusive Fizeau drag in spatiotemporal thermal metamaterials," *Phys. Rev. Lett.*, vol. 128, no. 14, p. 145901, 2022.

[5] A. M. Shaltout, V. M. Shalaev, and M. L. Brongersma, "Spatiotemporal light control with active metasurfaces," *Science*, vol. 364, no. 6441, pp. 1−10, 2019.

[6] S. Tessier Brothelande, *et al.*, "Experimental evidence of nonreciprocal propagation in space-time modulated piezoelectric phononic crystals," *Appl. Phys. Lett.*, vol. 123, no. 20, 2023, https://doi.org/10.1063/5.0169265.

[7] F. R. Morgenthaler, "Velocity modulation of electromagnetic waves," *IRE Trans. Microw. Theory Tech.*, vol. 6, no. 2, pp. 167−172, 1958.

[8] M. Mostafa, M. Mirmoosa, M. Sidorenko, V. Asadchy, and S. Tretyakov, "Temporal interfaces in complex electromagnetic materials: an overview," *Opt. Mater. Express*, vol. 14, no. 5, pp. 1103−1127, 2024.

[9] V. Bacot, M. Labousse, A. Eddi, M. Fink, and E. Fort, "Time reversal and holography with spacetime transformations," *Nat. Phys.*, vol. 12, no. 10, pp. 972−977, 2016.

[10] E. Lustig, *et al.*, "Time-refraction optics with single cycle modulation," *Nanophotonics*, vol. 12, no. 12, pp. 2221−2230, 2023.

[11] B. L. Kim, C. Chong, and C. Daraio, "Temporal refraction in an acoustic phononic lattice," *Phys. Rev. Lett.*, vol. 133, no. 7, p. 077201, 2024.

[12] J. T. Mendonça, "Time refraction and spacetime optics," *Symmetry*, vol. 16, no. 11, p. 1548, 2024.

[13] A. Shlivinski and Y. Hadad, "Beyond the Bode-Fano bound: wideband impedance matching for short pulses using temporal switching of transmission-line parameters," *Phys. Rev. Lett.*, vol. 121, no. 20, p. 204301, 2018.

[14] J. Mendonça, A. Martins, and A. Guerreiro, "Temporal beam splitter and temporal interference," *Phys. Rev. A*, vol. 68, no. 4, p. 043801, 2003.

[15] J. Mendonça, A. Guerreiro, and A. M. Martins, "Quantum theory of time refraction," *Phys. Rev. A*, vol. 62, no. 3, p. 033805, 2000.

[16] J. B. Pendry, "Air conditioning for photons," *Opt. Mater. Express*, vol. 14, no. 2, pp. 407−413, 2024.

[17] A. Akbarzadeh, N. Chamanara, and C. Caloz, "Inverse prism based on temporal discontinuity and spatial dispersion," *Opt. Lett.*, vol. 43, no. 14, pp. 3297−3300, 2018.

[18] N. Engheta, "Four-dimensional optics using time-varying metamaterials," *Science*, vol. 379, no. 6638, pp. 1190−1191, 2023.

[19] E. Galiffi, A. C. Harwood, S. Vezzoli, R. Tirole, A. Alù, and R. Sapienza, "Optical coherent perfect absorption and amplification in a time-varying medium," *arXiv preprint arXiv:2410.16426*, 2024.

[20] P. Tien, "Parametric amplification and frequency mixing in propagating circuits," *J. Appl. Phys.*, vol. 29, no. 9, pp. 1347−1357, 1958.

[21] V. Pacheco-Peña and N. Engheta, "Antireflection temporal coatings," *Optica*, vol. 7, no. 4, pp. 323−331, 2020.

[22] V. Pacheco-Peña and N. Engheta, "Temporal aiming," *Light Sci. Appl.*, vol. 9, no. 1, p. 129, 2020.

[23] S. A. Hilbert, C. Uiterwaal, B. Barwick, H. Batelaan, and A. H. Zewail, "Temporal lenses for attosecond and femtosecond electron pulses," *Proc. Natl. Acad. Sci.*, vol. 106, no. 26, pp. 10558−10563, 2009.

[24] P. Reck, C. Gorini, A. Goussev, V. Krueckl, M. Fink, and K. Richter, "Dirac quantum time mirror," *Phys. Rev. B*, vol. 95, no. 16, p. 165421, 2017.

[25] N. Goldman and J. Dalibard, "Periodically driven quantum systems: effective Hamiltonians and engineered gauge fields," *Phys. Rev. X*, vol. 4, no. 3, p. 031027, 2014.

[26] Z. Dong, H. Li, T. Wan, Q. Liang, Z. Yang, and B. Yan, "Quantum time reflection and refraction of ultracold atoms," *Nat. Photonics*, vol. 18, no. 1, pp. 68−73, 2024.

[27] F. Ok, A. Bahrami, and C. Caloz, "Electron scattering at a potential temporal step discontinuity," *Sci. Rep.*, vol. 14, no. 1, p. 5559, 2024.

[28] B. M. Bolotovskiĭ and V. L. Ginzburg, "The Vavilov-Cerenkov effect and the Doppler effect in the motion of sources with superluminal velocity in vacuum," *Sov. Phys. Usp.*, vol. 15, no. 2, p. 184, 1972.

[29] Z.-L. Deck-Léger, N. Chamanara, M. Skorobogatiy, M. G. Silveirinha, and C. Caloz, "Uniform-velocity spacetime crystals," *Adv. Photonics*, vol. 1, no. 5, p. 056002, 2019.

[30] J. B. Pendry, P. A. Huidobro, M. Silveirinha, and E. Galiffi, "Crossing the light line," *Nanophotonics*, vol. 11, no. 1, pp. 161−167, 2022.

[31] F. Biancalana, A. Amann, A. V. Uskov, and E. P. O'reilly, "Dynamics of light propagation in spatiotemporal dielectric structures," *Phys. Rev. E*, vol. 75, no. 4, p. 046607, 2007.

[32] I. Liberal, A. Ganfornina-Andrades, and J. E. Vázquez-Lozano, "Spatiotemporal symmetries and energy-momentum conservation in uniform spacetime metamaterials," *ACS Photonics*, vol. 11, no. 12, pp. 5273−5280, 2024.

[33] V. Granatstein, *et al.*, "Realization of a relativistic mirror: electromagnetic backscattering from the front of a magnetized relativistic electron beam," *Phys. Rev. A*, vol. 14, no. 3, p. 1194, 1976.

[34] M. Lampe, E. Ott, and J. H. Walker, "Interaction of electromagnetic waves with a moving ionization front," *Phys. Fluids*, vol. 21, no. 1, pp. 42−54, 1978.

[35] Y. Hadad and D. Sounas, "Space-time modulated loaded-wire metagratings for magnetless nonreciprocity and near-complete frequency conversion," *Opt. Mater. Express*, vol. 14, no. 5, pp. 1295−1308, 2024.

[36] S. Taravati, N. Chamanara, and C. Caloz, "Nonreciprocal electromagnetic scattering from a periodically space-time modulated slab and application to a quasisonic isolator," *Phys. Rev. B*, vol. 96, no. 16, p. 165144, 2017.

[37] N. A. Estep, D. L. Sounas, J. Soric, and A. Alù, "Magnetic-free non-reciprocity and isolation based on parametrically modulated coupled-resonator loops," *Nat. Phys.*, vol. 10, no. 12, pp. 923−927, 2014.

[38] Z.-L. Deck-Léger, A. Akbarzadeh, and C. Caloz, "Wave deflection and shifted refocusing in a medium modulated by a superluminal rectangular pulse," *Phys. Rev. B*, vol. 97, no. 10, p. 104305, 2018.

[39] S. Taravati and G. V. Eleftheriades, "Generalized space-time-periodic diffraction gratings: theory and applications," *Phys. Rev. Appl.*, vol. 12, no. 2, p. 024026, 2019.

[40] E. S. Cassedy and A. A. Oliner, "Dispersion relations in time-space periodic media: part I − stable interactions," *Proc. IEEE*, vol. 51, no. 10, pp. 1342−1359, 1963.

[41] E. S. Cassedy, "Dispersion relations in time-space periodic media: part II − unstable interactions," *Proc. IEEE*, vol. 55, no. 7, pp. 1154−1168, 1967.

[42] N. Chamanara, S. Taravati, Z.-L. Deck-Léger, and C. Caloz, "Optical isolation based on space-time engineered asymmetric photonic band gaps," *Phys. Rev. B*, vol. 96, no. 15, p. 155409, 2017.

[43] P. A. Huidobro, E. Galiffi, S. Guenneau, R. V. Craster, and J. B. Pendry, "Fresnel drag in space−time-modulated metamaterials," *Proc. Natl. Acad. Sci.*, vol. 116, no. 50, pp. 24943−24948, 2019.

[44] P. A. Huidobro, M. G. Silveirinha, E. Galiffi, and J. Pendry, "Homogenization theory of space-time metamaterials," *Phys. Rev. Appl.*, vol. 16, no. 1, p. 014044, 2021.

[45] K. A. Lurie, *An Introduction to the Mathematical Theory of Dynamic Materials*, New York, USA, Springer, 2007.

[46] N. Westerberg, S. Cacciatori, F. Belgiorno, F. Dalla Piazza, and D. Faccio, "Experimental quantum cosmology in time-dependent optical media," *New J. Phys.*, vol. 16, no. 7, p. 075003, 2014.

[47] E. J. Reed, M. Soljačić, and J. D. Joannopoulos, "Color of shock waves in photonic crystals," *Phys. Rev. Lett.*, vol. 90, no. 20, p. 203904, 2003.

[48] S. A. Fulling and P. C. Davies, "Radiation from a moving mirror in two dimensional space-time: conformal anomaly," *Proc. R. Soc. Lond.*, vol. 348, no. 1654, pp. 393−414, 1976.

[49] J. Sloan, N. Rivera, J. D. Joannopoulos, and M. Soljačić, "Controlling two-photon emission from superluminal and accelerating index perturbations," *Nat. Phys.*, vol. 18, no. 1, pp. 67−74, 2022.

[50] A. Bahrami, Z.-L. Deck-Léger, Z. Li, and C. Caloz, "A generalized FDTD scheme for moving electromagnetic structures with arbitrary space-time configurations," *IEEE Trans. Antenn. Propag.*, vol. 72, no. 2, pp. 1721−1734, 2024.

[51] A. Bahrami and C. Caloz, "Electrodynamics of accelerated space-time engineered-modulation metamaterials," in *2023 Metamaterials*, IEEE, 2023, pp. X−031.

[52] A. Bahrami, Z.-L. Deck-Léger, and C. Caloz, "Electrodynamics of accelerated-modulation space-time metamaterials," *Phys. Rev. Appl.*, vol. 19, no. 5, p. 054044, 2023.

[53] C. Caloz and Z.-L. Deck-Léger, "Spacetime metamaterials − part I: general concepts," *IEEE Trans. Antenn. Propag.*, vol. 68, no. 3, pp. 1569−1582, 2019.

[54] C. Caloz and Z.-L. Deck-Léger, "Spacetime metamaterials − part II: theory and applications," *IEEE Trans. Antenn. Propag.*, vol. 68, no. 3, pp. 1583−1598, 2019.

[55] R. Bellman, R. Kalaba, and S. Ueno, "Invariant imbedding and scattering of light in a one-dimensional medium with a moving boundary," *J. Math. Anal. Appl.*, vol. 15, no. 2, pp. 171−182, 1966.

[56] C. Tsai and B. Auld, "Wave interactions with moving boundaries," *J. Appl. Phys.*, vol. 38, no. 5, pp. 2106−2115, 1967.

[57] A. Ishimaru, *Electromagnetic Wave Propagation, Radiation, and Scattering: From Fundamentals to Applications*, Hoboken, New Jersey, John Wiley & Sons, 2017.

[58] L. A. Ostrovskii and B. A. Solomin, "Correct formulation of the problem of wave interaction with a moving parameter jump," *Radiophys. Quantum Electron.*, vol. 10, no. 8, pp. 666−668, 1967.

[59] Z.-L. Deck-Léger and C. Caloz, "Scattering at interluminal interface," in *2019 AP-S*, IEEE, 2019, pp. 367−368.

[60] See Supplementary Material at [URL will be inserted by publisher] for the detailed derivation of the equations in the text.

[61] J. Van Bladel, *Relativity and Engineering*, vol. 15, Heidelberg, Germany, Springer Science & Business Media, 2012.